Chapter 2

Geologic History of West Texas

Kevin Urbanczyk[1], David Rohr[1], and John C. White[1]

Introduction

The region embraced within the Trans-Pecos region of Texas encompasses many snapshots of North American geologic history. Precambrian crystalline metamorphic rocks are exposed in the Franklin Mountains, Van Horn Mountains, and Sierra Diablo Mountains. Xenoliths of these rocks recovered from volcanic rocks in the Davis Mountains, Bofecillos Mountains, and Chisos Mountains provide strong evidence that almost all of Trans-Pecos Texas is underlain by Precambrian rocks similar to those that crop out at the surface. Cambrian to Pennsylvanian rocks crop out in the Franklin Mountains, Marathon Basin, Solitario, and at Persimmon Gap. These rocks represent a transgressive, then regressive, marine sequence that was caught between the North American continent and another unidentified continent during the Pennsylvanian and intensely deformed and thrust onto North America forming the Marathon-Ouachita Mountains. The foreland basin of these mountains became the Permian Basin, and the carbonate rocks associated with this intracratonic sea now crop out in the Guadalupe, Glass, Apache, Van Horn, and Sierra Diablo mountain ranges. A depositional hiatus from the Triassic to Mid-Cretaceous was followed by the deposition of Mid- to Late-Cretaceous limestone that covers much of central and west Texas and frequently hosts important aquifers. From the Late Cretaceous to the Early Tertiary, these rocks were locally deformed during the Laramide Orogeny, which can be seen in the Del Norte-Santiago Mountains, Mariscal Mountain, the Terlingua-Fresno Monocline, and in the Chihuahua Tectonic Belt. Laramide compression was followed by a long period of large-scale ignimbritic volcanism in Trans-Pecos Texas. As compression continued to wane, ignimbritic volcanism yielded to smaller-scale effusive volcanism that was coupled with extensional tectonics, resulting in Basin and Range structures and related mountain ranges in the Trans-Pecos. Between these ranges, which include the Franklin, Hueco, Guadalupe, Delaware, Sierra Diablo, Sierra Vieja, and Van Horn mountains, large basins formed that filled with thick sequences of gravel and sand eroded from the adjacent mountains. It is in this setting that we presently reside.

[1] Department of Earth and Physical Sciences, Sul Ross State University

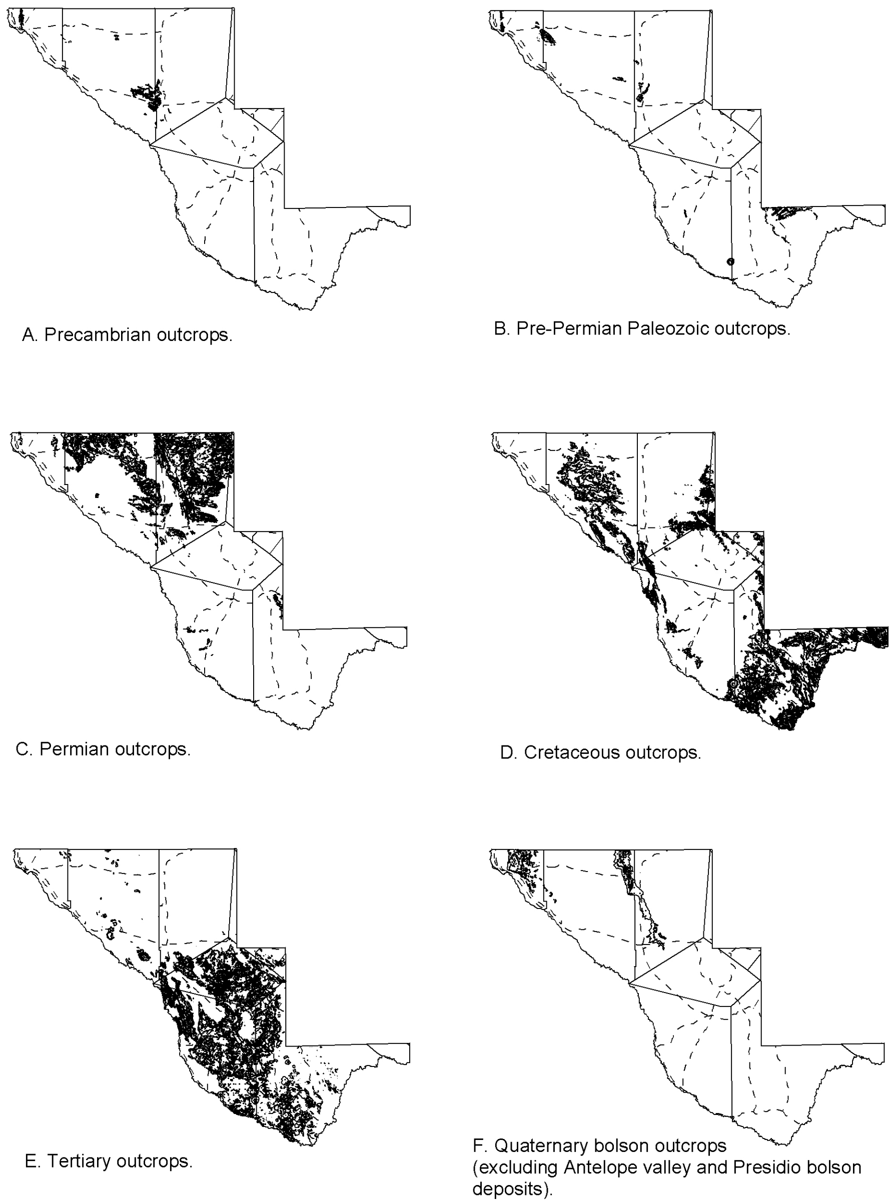

Figure 2-1: Geologic maps of time intervals discussed in the text.

Precambrian Geology

Precambrian metamorphic rocks crop out only near Van Horn and El Paso (fig. 2-1). The rocks have been interpreted to represent igneous and sedimentary rocks associated with an island arc system that were metamorphosed and accreted to the margin of North America during collision with an unknown continent. These rocks are coeval with the Llano terrane of Central Texas, which also formed during the Grenville orogeny, at approximately 1 billion years ago.

Paleozoic Geology

Although Paleozoic strata underlie most of Trans-Pecos Texas, they crop out only in a few regions (fig. 2-1). These can be broadly divided into the Paleozoic shelfal facies in the El Paso and Van Horn areas, the basinal (or geosynclinal) Marathon facies, and the Permian intracratonic basinal facies in the Guadalupe Mountains southward through the Sierra Diablo and Apache Mountains, the Glass Mountains, and the Shafter-Pinto Canyon area.

Paleozoic Facies and Tectonics

What is now the Trans-Pecos was situated along the south margin of the North American continent (Laurentia) during early Paleozoic time. The El Paso and Van Horn areas were the site of deposition of limestone, dolomite, and sandstone in a shallow, tropical sea located near the edge of the continental shelf (Stoudt, 1996). The strata in these areas were slightly deformed during Mesozoic and Cenozoic uplift, resulting in the beds being tilted from horizontal. The Franklin Mountains are a good example of a block-faulted mountain range.

Lower Paleozoic sandstone and limestone unconformably overlie Precambrian granite and metamorphic rocks in the El Paso and Van Horn areas. In the Sierra Diablo, late Paleozoic uplift has resulted in the older Paleozoic rocks being stripped off, and upper Paleozoic rocks lie unconformably over Precambrian.

In contrast, the Paleozoic rocks in the Marathon Basin have very different lithologies and have been folded and faulted to a much greater degree. These rocks, exposed in the Marathon Basin and in the Solitario to the southwest, are part of the Ouachita Orogenic Belt. The strata were originally deposited as shales, cherts, and turbidite sandstones in a deep oceanic setting south of the North American continent and represent one of the longest intervals of essentially continuous deposition known (King, 1978). At the close of the Paleozoic, the south margin of North America collided with South America (then part of Gondwanaland), and the rocks were deformed and thrust northward over the North American platform margin. Folding and thrust faults (fig. 2-2) result in some wells penetrating distinctive units such as the Caballos Novaculite (Folk and McBride, 1978) several times in one borehole.

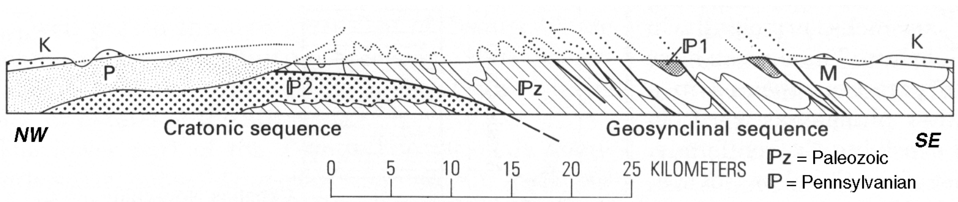

Figure 2-2: Cross section of the Marathon Basin showing the complex structure. Deformation near the rocks during the Ouachita Orogeny end of the Paleozoic caused extensive folding and faulting when geosynclinal facies were thrusted over cratonic (modified from King, 1981).

The Permian Basin

Up to 3,000 m of Permian rocks underlies much of West Texas and southeastern New Mexico. Because of prolific oil production, the stratigraphy of the West Texas or Permian Basin has been studied in great detail (Hill, 1996). Subsurface information in the forms of well logs and seismic profiles is available for most of the area. The Permian Basin can be thought of as a small but deep inland sea that developed in a sag of the North American continental crust after collision of the continent with Gondwanaland.

The earliest oil drilling in the Permian Basin revealed that the basin actually consists of three smaller basins: the Midland, Delaware, and Marfa Basins. During the Permian Period, these basins were enclosed marine basins accumulating organic-rich sediments. The edges of the two basins in Trans-Pecos Texas (the Delaware and Marfa Basins) were partly surrounded by massive limestone reefs. Parts of the reef can now been seen at the surface in the Guadalupe Mountains, including the peak of El Capitan. The margins of the basins are characterized by rapid lithologic facies changes. The basinal facies are bedded shales and sandstones, the reef is massive limestone, and the back reef is commonly dolomite. A small amount of Permian gypsum, the Castile Formation, is exposed near the Texas-New Mexico border. Permian strata were uplifted to their present elevation during the Cenozoic, and have been subjected to relatively minor deformation, mostly normal faulting (fig. 2-3).

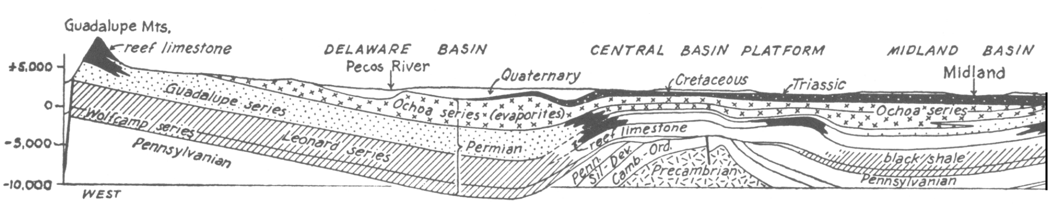

Figure 2-3: Cross section of the Permian Basin. Most of the structural features were present during the Permian and controlled the sedimentary facies (modified from King, 1959).

Mesozoic Geology

The paucity of Triassic and Jurassic rocks in Trans-Pecos Texas either at the surface or in the subsurface strongly suggests that this region was subaerially exposed during these periods and experienced no active tectonism (McCormick and others, 1996). In adjacent northern Chihuahua, however, rifting and subsidence of the Chihuahua Trough related to the opening of the Gulf of Mexico and Atlantic Ocean began during the Middle Jurassic. Triassic rocks are lacking throughout the Trans-Pecos area and adjacent Chihuahua. Jurassic rocks have been mapped at the surface only in the Malone Mountains, near Sierra Blanca (Albritton and Smith, 1965) and in the subsurface in the Chihuahua Trough (Henry and Price, 1985). Widespread clastic and carbonate sedimentation did not begin in the Trans-Pecos until the Middle Cretaceous with the deposition of the Comanchean series rocks, which represent primarily carbonate sedimentation associated with a widespread, intracontinental sea that inundated much of North America from Texas to Alberta (fig. 2-1). Late Cretaceous uplift related to the Laramide orogeny is responsible for Gulfian series rocks, a regressive sequence of limestone to terrigenous shales and sandstones that overlie the Comanchean series.

Comanchean deposition began with a coarse-grained, basal conglomerate consisting of clasts of Paleozoic rocks. This conglomerate unconformably overlies the Pennsylvanian Tesnus Formation, where it is exposed in the Solitario, Big Bend Ranch State Park, and at Persimmon Gap, Big Bend National Park. In the Solitario, it is mapped separately as the Shutup Conglomerate; in Big Bend National Park, it is mapped as a lower part of the Glen Rose Limestone (McCormick and others, 1996). The Glen Rose Limestone is overlain by the Del Carmen Limestone, which is equivalent to the Edwards Limestone in Central Texas. Completing the Comanchean (Lower Cretaceous) series in West Texas above the Del Carmen Limestone are the Sue Peaks Formation (equivalent to the Kiamichi Formation) and the Santa Elena Limestone (equivalent to the Georgetown Limestone) (Maxwell and others, 1967; McCormick and others, 1996). The Comanchean series is overlain by the Gulfian series, a regressive sequence beginning with the Del Rio Clay, followed by the Buda Limestone, and the Boquillas, Pen, Aguja, and Javelina Formations.

Cenozoic Geology

Sedimentation from the Late Cretaceous into the Early Tertiary was nearly continuous and shows a regressive sequence of marine limestone yielding to swampy shale and terrigenous sandstone (Maxwell and others, 1967). This sedimentation was contemporaneous with the compressive Laramide orogeny, which uplifted long, linear mountain chains (including the Del Norte-Santiago Mountains and the Chihuahua Tectonic belt) and was the most likely cause of the retreat of the epeiric seas in Trans-Pecos Texas (Lehman, 1986).

The Laramide orogeny, lasting from about 100 to 50 million years ago (Ma), began with the onset of subduction of the Farallon plate under the North American plate (Coney and Reynolds, 1977; McDowell and Clabaugh, 1979). Laramide compression produced folds, thrust faults, and high-angle reverse faults; shortened Trans-Pecos Texas about 3.4 percent; and reactivated west-northwest-striking, left-lateral strike slip basement faults (Barker, 1987). Laramide features in the Trans-Pecos include the Terlingua-Fresno monocline, Mariscal Mountain, the Del Norte-Santiago Mountains, and the Chihuahua Tectonic Belt (Muehlberger and Dickerson, 1989). Laramide compression peaked in the Late Paleocene and ended during the Eocene (Coney and Reynolds, 1977; Price and others, 1987). Magmatism began during the Eocene (~48 Ma) as compressive stresses began to wane and continued through the Oligocene and into the Miocene, ending about 17 Ma (Henry and McDowell, 1986).

Early magmatism began with the emplacement of a suite of intrusive rocks in the El Paso area around 48 Ma and was followed by activity in the Christmas Mountains and western Big Bend National Park between 45 and 40 Ma. Large-scale silicic volcanism began in the Davis Mountains and Sierra Vieja about 39 Ma and continued until about 35 Ma. The Crossen Trachyte and Star Mountain Rhyolite are generally accepted to be the oldest volcanic units within the Davis Mountains, erupting from unknown sources about 38.6 Ma (Henry and others, 1994). The Buckhorn caldera, the first recognized caldera in the Davis Mountains, formed about the same time, with the eruption of the Gomez Tuff (Parker, 1986). Volcanism was nearly contemporaneous in the Sierra Vieja and Van Horn Mountains, with the eruption of the Buckhorn Ignimbrite from unknown sources and the eruption of the Chambers and High Lonesome Tuffs from the Van Horn caldera (Henry and Price, 1986). The Solitario laccocaldera also erupted during this initial phase. In the southern Davis Mountains, several widespread flows of mafic to intermediate lavas erupted, producing the lavas of the Pruett Formation, including the Sheep Canyon Basalt, Potato Hill Andesite, and Cottonwood Springs Basalt. This activity was followed by the formation of the Paisano volcano, a large trachyte-rhyolite shield volcano, around 36 Ma (Parker, 1983). The Eagle Mountain and Quitman Mountain calderas are approximately contemporaneous with the Paisano volcano (Henry and Price, 1984). Large-scale volcanism in the Davis Mountains ended with the eruption of the Barrel Springs and Wild Cherry Formations from the Paradise Mountain–Pine Peak caldera between 36.4 and 35.4 Ma (Henderson, 1979).

Following the cessation of activity in the Davis Mountains, volcanism shifted southward to Big Bend National Park and the Chinati Mountains. The earliest known episode of volcanism in Big Bend National Park is represented by the 47 to 40 Ma Alamo Creek Basalt. Magmatism in Big Bend resumed between 35 and 32 Ma with the eruption of lavas and tuffs of the Chisos Group, followed by those of the South Rim Formation. From the Chinati Mountains area, lavas and tuffs of the Shelly Group and Morita Formation were erupted from unknown sources between 34 and 32 Ma. Between 33 and 32 Ma, the Chinati Mountains caldera formed as a result of the eruption of the Mitchell Mesa Tuff, the largest (>1000 km^3) ash-flow tuff in Trans-Pecos Texas. This eruption was followed by several hundreds of thousand years of continued volcanic activity that resulted in the accumulation of a large volcaniclastic alluvial apron around the Chinati Mountains, which is represented by the Tascotal Formation.

During the Oligocene, between 31 and 28 Ma, the compressive stress regime yielded to a tensional (extensional) environment, which persisted through the remainder of the

Cenozoic (Muehlberger and others, 1978; Henry and others, 1991). Volcanism during this phase was restricted to Big Bend Ranch State Park and adjacent Mexico and began with the eruption of the San Carlos and Santana Tuffs from the Sierra Rica caldera complex in northern Mexico at 30 and 27.8 Ma. Volcanism continued between 27.8 and 26 Ma with the eruption of the Rawls Formation, a complex series of mostly mafic to intermediate lavas. Faulting associated with extensional tectonics produced a discontinuous series of north-northwest-trending pull-apart grabens that terminate at west-northwest-trending strike-slip faults (Barker, 1987). Mafic volcanism closely associated with faulting continued until about 17 Ma.

References

Albritton, C. C., Jr., and Smith, J. F., Jr., 1965, Geology of the Sierra Blanca area, Hudspeth County, Texas: U.S. Geological Survey Professional Paper 479, 131 p.

Barker, D. S., 1987, Tertiary alkaline magmatism in Trans-Pecos Texas: *in* Geological Society of America Special Publication No. 30, p. 415-431.

Coney, P. J., and Reynolds, S. J., 1977, Cordilleran benioff zones: Nature, v. 270, p. 403-406.

Folk, R. L., and McBride, E. F., 1978, Origin of the Caballos Novaculite: *in* Mazzullo, S. J., ed., Tectonics and Paleozoic facies of the Marathon Geosyncline, West Texas: Permian Basin Section, SEPM, Publication no. 78-17, p. 101-130.

Henderson, G., 1979, Geology of the Medley Kaolin deposits and associated volcanic rocks, Jeff Davis County, Texas. Unpublished M.S. thesis, Baylor University, Waco, Texas, p. 186.

Henry, C. D., Kunk, M. J., and McIntosh, W. C., 1994, ^{40}Ar/^{39}Ar chronology and volcanology of silicic volcanism in the Davis Mountains, Trans-Pecos Texas: Geological Society of America Bulletin, v. 106, p. 1359-1376.

Henry, C. D., and McDowell, F. W., 1986, Geochronology of magmatism in the Tertiary volcanic field, Trans-Pecos Texas: *in* Price, J. G., Henry, C. D., Parker, D. F., and Barker, D. S., eds., Igneous geology of Trans-Pecos Texas–Field trip guide and research articles: The University of Texas at Austin, Bureau of Economic Geology Guidebook 23, p. 99-122.

Henry, C. D., and Price, J. G., 1984, Variations in caldera development in the Tertiary volcanic field of Trans-Pecos Texas: Journal of Geophysical Research, v. 91, p. 6213-6224.

Henry, C. D., and Price, J. G., 1985, Summary of the tectonic development of Trans-Pecos Texas: The University of Texas at Austin, Bureau of Economic Geology, Miscellaneous Map No. 36, p 7.

Henry, C.D. and Price, J.G., 1986, Early Basin and Range development in Trans-Pecos Texas and adjacent Chihuahua: Magmatism and orientation, timing, and style of extension, Journal of Geophysical Research, v. 91, p. 6213-6224.

Henry, C.D., Price, J.G., and James, E.W., 1991, Mid-Cenozoic stress evolution and magmatism in the southern Cordillera, Texas and Mexico: Transition from continental arc to intraplate extension, Journal of Geophysical Research, v. 96, p. 13545-13560.

Hill, C. A., 1996, Geology of the Delaware Basin: Permian Basin Section, SEPM, Publication 96-39, p. 480.

King, P. B., 1959, The evolution of North America: Princeton University Press, 190 p.

King, P. B., 1978, Tectonics and sedimentation of the Paleozoic rocks in the Marathon region, West Texas: *in* Mazzullo, S. J., ed., Tectonics and Paleozoic facies of the Marathon Geosyncline, West Texas: Permian Basin Section, SEPM, Publication No. 78-17, p. 5-38.

King, P. B., 1981, Geology of the eastern part of the Marathon Basin, Texas: U.S. Geological Survey Professional Paper 1157, 40 p. [1980 FIG. 2.2]

Lehman, T. M., 1986, Late Cretaceous sedimentation in Trans-Pecos Texas: *in* Pause, P. H. and Spears, R. G., eds., Geology of the Big Bend area and Solitario dome, Texas: West Texas Geological Society 1986 Field Trip Guidebook, p. 105-110.

Maxwell, R. A., Lonsdale, J. T., Hazzard, R. T., and Wilson, J. A., 1967, Geology of Big Bend National Park, Brewster County, Texas: The University of Texas at Austin, Bureau of Economic Geology, Publication 6711, 320 p.

McCormick, C. L., Smith, C. I., and Henry, C. D., 1996, Cretaceous stratigraphy: *in* Henry, C. D. and Muehlberger, W. R., eds., Geology of the Solitario dome, Trans-Pecos Texas: Paleozoic, Mesozoic, and Cenozoic sedimentation, tectonism, and magmatism: The University of Texas at Austin, Bureau of Economic Geology Report of Investigations No. 240, p. 30-46.

McDowell, F. W., and Clabaugh, S. E., 1979, Ignimbrites of the Sierra Madre Occidental and their relation to the tectonic history of western Mexico: *in* Geological Society of America Special Publication 180, p. 113-124.

Muehlberger, W. R., Belcher, R. C., and Goetz, L. K., 1978, Quaternary faulting in Trans-Pecos Texas: Geology, v. 6, p. 337-340.

Muehlberger, W. R., and Dickerson, P. W., 1989, A tectonic history of Trans-Pecos Texas: *in* Muehlberger, W. R., and Dickerson, P. W., eds., Structure and stratigraphy of Trans-Pecos Texas: American Geophysical Union Field Trip Guidebook T317, p. 35-54.

Parker, D.F., 1983. Origin of the trachyte-quartz trachyte-peralkalic rhyolite suite of the Oligocene Paisano volcano, Trans-Pecos Texas. Geological Society of America Bulletin, v. 94, p. 614-629.

Parker, D.F., 1986. Stratigraphy, structural, and petrologic development of the Buckhorn caldera, northern Davis Mountains, Trans-Pecos Texas, *in* Price, J.G., Henry, C.D., Parker, D.F., and Barker, D.S., eds., Igneous geology of Trans-Pecos Texas: Field trip guide and research articles. The University of Texas at Austin Bureau of Economic Geology Guidebook 23, p. 286-302.

Price, J. G., Henry, C. D., Barker, D. S., and Parker, D. F., 1987, Alkalic rocks of contrasting tectonic settings in Trans-Pecos Texas: Geological Society of America Special Paper 215, p. 335-346.

Stoudt, E. L., ed., 1996, Precambrian-Devonian geology of the Franklin Mountains, West Texas–analogs for exploration and production in Ordovician and Silurian karsted reservoirs in the Permian Basin: West Texas Geological Society, Publication 96-100, p. 117-123.

Chapter 3

Evaluation of Groundwater Recharge in Basins in Trans-Pecos Texas

Bridget R. Scanlon[1], Bruce K. Darling[2], and William F. Mullican III[3]

Introduction

The Trans-Pecos Texas region, in the southeast part of the Basin and Range province, consists of topographically high plateaus and mountains separated by major normal faults from adjacent, topographically low desert basins. The basins were progressively filled by detritus eroded from adjacent ranges and from Colorado and New Mexico by the ancestral Rio Grande (Gustavson, 1990). The study area includes the Diablo Plateau, Hueco Bolson, and Eagle Flat and Red Light Basins (fig. 3-1). Depth to groundwater ranges from 100 to 900 ft (30 to 274 m) beneath the Diablo Plateau, 350 to 500 ft (107 to 152 m) in the Hueco Bolson, 100 to 1,100 ft (30 to 335 m) in Eagle Flat Basin, and 10 to 500 ft (3 to 152 m) in Red Light Basin.

Trans-Pecos Texas lies within the northern Chihuahuan Desert (King, 1948). The region has a subtropical, arid climate (Larkin and Bomar, 1983). Long-term average annual precipitation ranges from 11 inches (280 mm) in Hueco Bolson to 12.6 inches (320 mm) in Sierra Blanca in Eagle Flat and Red Light Basins. Most precipitation occurs in the summer months as thunderstorms.

The geology of the different regions is quite variable. The Diablo Plateau site consists of shallow alluvium over Cretaceous limestone. The Hueco Bolson is made up of about 0 to 75 ft (~0 to 23 m) of coarse-grained material over 600 ft (183 m) of clay interbedded with silts and sands. Basin-fill deposits in the Eagle Flat region are generally fine grained muds, which are overlain by sand sheets in some parts of the basin.

Methods

The theoretical basis for the various techniques used to evaluate groundwater recharge in the study area is described next in order to provide the reader with a conceptual understanding of the different approaches. We used physical, chemical, and isotopic data from the unsaturated zone to determine whether groundwater recharge was occurring on

[1] Bureau of Economic Geology
[2] L.B.G. Guyton and Associates
[3] Texas Water Development Board

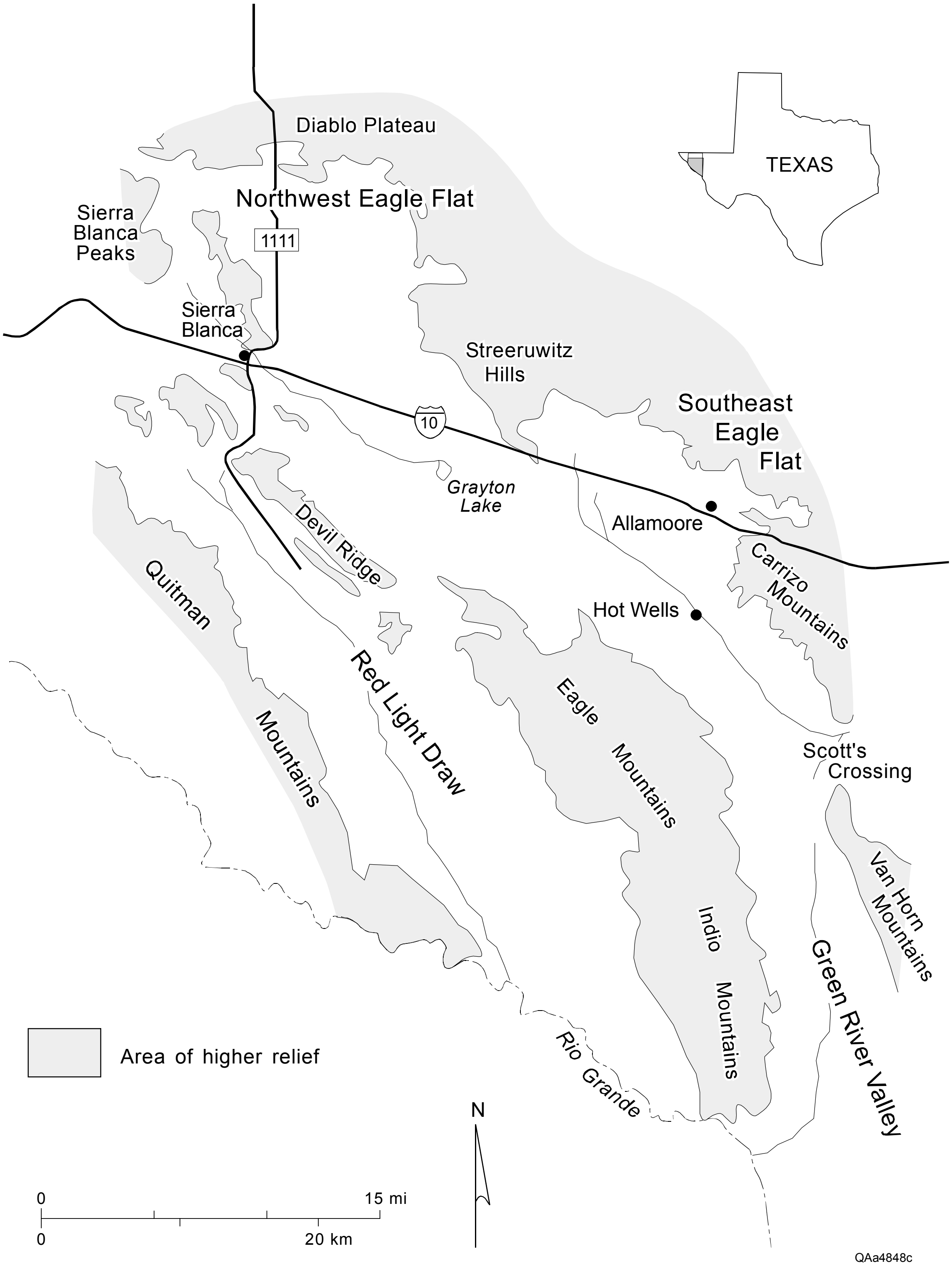

Figure 3-1: Location of the study area, including Diablo Plateau and Hueco Bolson and Eagle Flat and Red Light Basins.

the valley floors and on the Diablo Plateau. The unsaturated zone is the zone between the land surface and the water table, where pore spaces are filled with water and air. Water pressures are negative in the unsaturated zone and positive in the saturated zone. Physical data were used to determine the direction of water movement at a site. Chemical and isotopic tracers were used to quantify net water fluxes over long time periods. Groundwater tracers were also used on the Diablo Plateau and in the Eagle Flat and Red Light Basins to evaluate recharge.

Direction of Water Movement

Increasing potential energy with depth in the subsurface in the study area indicates that water is moving upward and that there is no recharge there. We can understand this concept by considering the gravitational force field, which is related to elevation of an object relative to a datum. Gravitational potential energy increases with elevation above a datum, such as the land surface, and objects will move from higher to lower gravitational potential energy (i.e., from higher to lower elevations). In soils, potential energy is related to forces in the soil, such as capillary, adsorptive, and osmotic forces (water-potential energy), and water will move from regions of high to low potential energy. Energy can be expressed in different units such as pressure (mega Pascals [Mpa] bars, or atmospheres) or head (ft, m). One MPa is equivalent to 10 bars, or 102 m. Thermocouple psychrometers were used to measure the relative humidity of the soil air, which was converted to matric potential energy according to the Kelvin equation.

Chemical and Isotopic Tracers

Chloride concentrations in unsaturated-zone pore water have been used to study recharge in semiarid systems over time scales ranging to thousands of years. Chloride concentrations in unsaturated-zone pore water are inversely proportional to water flux: high chloride concentrations in pore water indicate low water fluxes because chloride accumulates in the unsaturated zone as a result of evapotranspiration. In contrast, low chloride concentrations indicate high water flux because chloride is flushed through the unsaturated zone. The recharge rate, or water flux, is calculated by dividing the chloride input (precipitation × chloride concentration in precipitation) by the chloride concentration in the unsaturated zone. The age represented by chloride at any depth can be estimated by dividing the total amount of chloride from the surface to that depth by the annual chloride input.

Chlorine-36, a radioactive isotope of chlorine, has been used to a limited extent to date pore water in arid unsaturated zones. Chlorine-36 (^{36}Cl), which is produced naturally in the atmosphere (Bentley and others, 1986), has a half-life of 301,000 yr. The term *half-life* refers to the amount of time required for one-half of the atoms of a radioactive element to decay to half of the initial value. Nuclear-weapon tests conducted in the Pacific between 1952 and 1958 resulted in ^{36}Cl concentrations in rainfall that were as much as 1,000 times greater than natural fallout levels (fig. 3-2; Bentley and others, 1986). Bomb-pulse ^{36}Cl:Cl ratios have been used to estimate water fluxes during the past 40 yr and to evaluate preferential flow (Phillips and others, 1988; Scanlon, 1992;

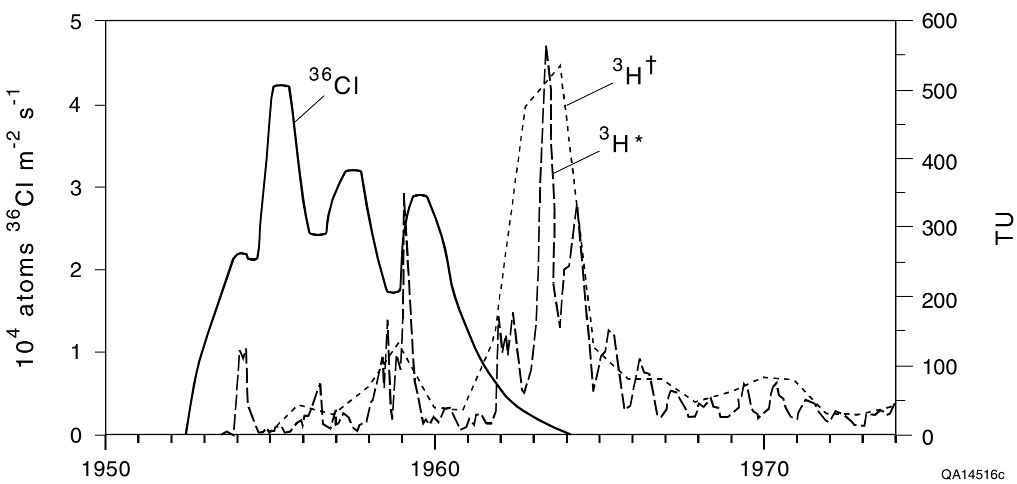

Figure 3-2: Temporal variations in ^3H and ^{36}Cl fallout from Ottawa, Canada (Scanlon, 1992).

Fabryka-Martin and others, 1993) (fig. 3-1). The depth of this high concentration of $^{36}Cl:Cl$ ratios in the soil water can be used to estimate how far water has moved during the time between bomb-pulse fallout and soil-sample collection (~ 40 yr). Radioactive decay of ^{36}Cl can also be used to estimate water ages to 1 million yr.

Tritium (^3H), a radioactive isotope of the element hydrogen (H) and produced naturally in the upper atmosphere, results in concentrations in precipitation over the northern hemisphere of 1 to 20 tritium units (TU) (Michel, 1989; Solomon and Sudicky, 1991) and averages approximately 5 TU (Mazor, 1991, p. 151). We define 1 TU as one atom of ^3H in 10^{18} atoms of H, and the half-life of ^3H is 12.43 yr. Tritium concentrations increased from 10 to ≥ 2,000 TU during atmospheric nuclear testing (IAEA, 1983) that began in 1952 and peaked in 1963 to 1964 (fig. 3-2). Tritium generated by the above-ground detonations of nuclear weapons is referred to as *bomb-pulse tritium*. Tritium that recharged groundwater in 1953 would have decayed to less than 0.5 TU by 2001, assuming an initial average value of 5 TU. Therefore, tritium concentrations of less than 0.5 TU are often interpreted to indicate recharge before 1952, and higher levels of tritium are regarded as indicative of post-1952 recharge. Subsurface distribution of bomb-pulse tritium in the unsaturated zone can be used to estimate how deep water has moved in the past 40 yr—a procedure similar to the one described for ^{36}Cl.

Carbon-14 (^{14}C), a radioactive isotope of carbon, is formed naturally in the upper levels of the atmosphere. Because of its long half-life, ^{14}C can be used to date groundwater with recharge ages to 10,000 yr. The concentration of ^{14}C is reported as percent modern carbon (pmc), which is the ratio of ^{14}C in a sample of groundwater measured against the concentration in an internationally accepted standard of oxalic acid. The apparent age of a water sample is inversely related to the concentration of ^{14}C. A value of 100 pmc indicates modern water. A value of 50 pmc represents an apparent age of 1 half-life, or 5,730 yr.

Stable isotopes of oxygen (^{18}O) and hydrogen (^{2}H, or deuterium) have been used to evaluate unsaturated flow. Because of coupling between fractionation of oxygen and hydrogen, a plot of stable isotopes of water samples from precipitation, rivers, and lakes throughout the world follows a straight line called the *global meteoric water line* (Craig, 1961).

Although the isotopic composition of individual rain events is highly variable, the annual mean values are fairly constant (Gat, 1981). The isotopic composition of pore water in the unsaturated zone is generally either depleted or enriched relative to the mean isotopic composition of rainwater. Enriched values of the stable isotopes relative to the meteoric water line indicate evaporation from surface water before infiltration or from pore water in the unsaturated zone. Slopes of ^{2}H versus ^{18}O are about 5 for surface-water evaporation but can decrease to 2 for evaporation of pore water in the unsaturated zone (Allison, 1982).

Field and Laboratory Methods

Sediment samples were collected for water-potential measurements in the laboratory from 8 boreholes to 46-ft (14-m) depth in the Hueco Bolson and 48 boreholes to 102-ft (31-m) depth in Eagle Flat Basin (Scanlon and others, 1991, 2000). The boreholes were drilled by using a hollow-stem auger, and samples were collected in split-tube core barrels (1.5 m [4.9 ft] long). To monitor water-potential variations, field psychrometers were installed in two locations in the Hueco Bolson and in one location in Eagle Flat Basin.

Sediment samples were collected from 10 boreholes to 31.5-ft (9.6-m) depth on the Diablo Plateau, 10 boreholes to 73.5-ft (22.4-m) depth in Hueco Bolson, and 52 boreholes to 102-ft (31-m) depth in Eagle Flat Basin for laboratory determination of chloride content (fig. 3-1). $^{36}Cl:Cl$ ratios and ^{3}H were measured in soil samples collected in a shallow pit in Hueco Bolson and in five boreholes in Eagle Flat Basin. Samples for $^{36}Cl:Cl$ were analyzed by Accelerator Mass Spectrometry at Lawrence Livermore National Laboratory. Samples for ^{3}H from Hueco Bolson were analyzed unenriched at the University of Waterloo, and those from Eagle Flat Basin were analyzed, enriched by standard direct scintillation methods, at the University of Arizona Tritium Laboratory or by gas proportional counting at the University of Miami Tritium Laboratory. Samples from seven boreholes in Eagle Flat Basin were analyzed for stable isotopes of hydrogen (^{2}H) and oxygen (^{18}O). The analyses were done by the Desert Research Institute (University of Nevada, Las Vegas).

Groundwater samples were collected from 30 wells on the Diablo Plateau for ^{3}H analysis. A total of 74 samples were collected from 59 wells in Eagle Flat and Red Light Basins for ^{14}C and ^{3}H analyses.

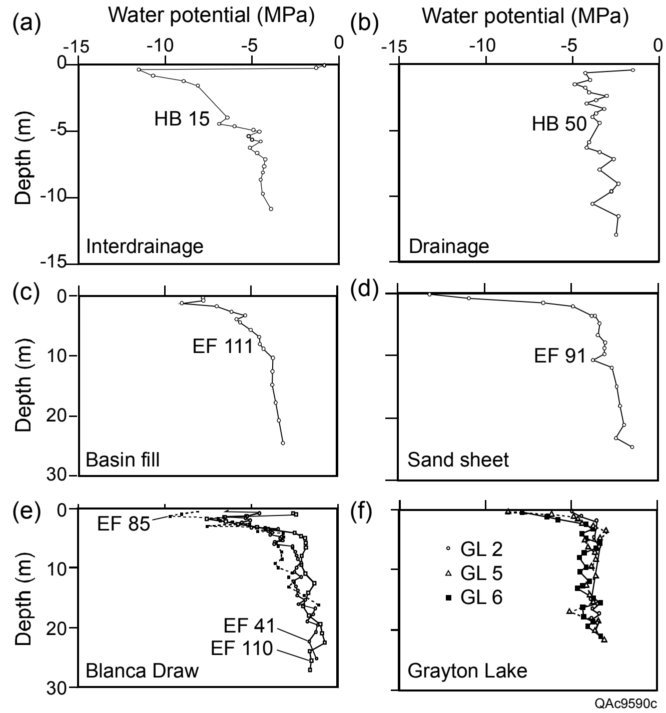

Figure 3-3: Typical water-potential profiles in (a, b) Hueco Bolson (interdrainage area, HB 15, drainage area, HB 50) and in (c–f) Eagle Flat Basin (interdrainage mud flats [EF 111], interdrainage sand sheet [EF 91], Blanca Draw [EF 41, 85, 110], and Grayton Lake [GL 2, 5, and 6]).

Results

Valley-Floor Settings in the Hueco Bolson and Eagle Flat Basin

Measured water potentials in interdrainage areas were extremely low in the Hueco Bolson and Eagle Flat Basin, indicating that the sediments are dry (Scanlon and others, 1991, 2000) (fig. 3-3). Water potential generally increased with depth, suggesting that water is moving upward in the profile as a result of long-term drying. Long-term monitoring of water potentials in the Hueco Bolson and Eagle Flat Basin in interdrainage areas indicates that during the past 7 to 10 yr, water did not move below the top 3 ft in a sandy location in Hueco Bolson or below 1 ft in a silt-loam site in the Hueco Bolson or a similar site in Eagle Flat Basin. Drainage areas in the Hueco Bolson and Eagle Flat Basin (Blanca Draw) also had low water potentials and upward gradients indicating upward water movement. The drainage areas are generally characterized by vegetation, such as mesquite, that can readily remove water from the subsurface and dry out the soil profile. However, water potentials at depths of more than 15 to 30 ft beneath Blanca Draw were much higher than those in adjacent regions, indicating downward water movement at these depths. Water potentials beneath Grayton Lake playa in Eagle Flat Basin were also

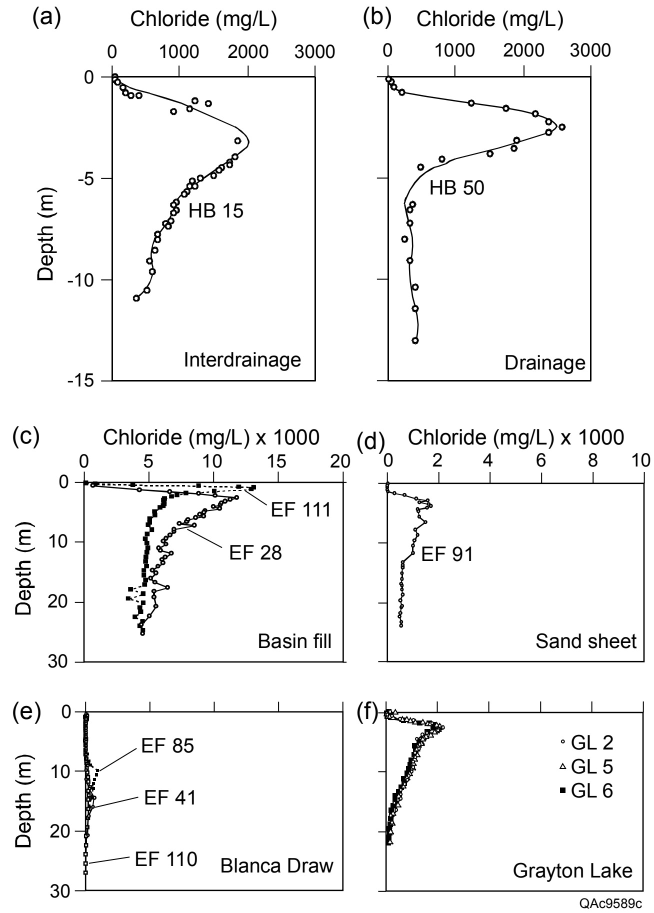

Figure 3-4: Typical chloride profiles in (a, b) Hueco Bolson (interdrainage area, HB 15; drainage area, HB50) and in (c–f) Eagle Flat Basin (interdrainage basin fill [EF 28, 111], interdrainage sand sheet [EF 91], Blanca Draw [EF 41, 85, and 110], and Grayton Lake [GL 2, 5, and 6]).

low, indicating dry conditions. Recent studies indicate that these upward water-potential gradients in interdrainage areas may take thousands of years to develop, and these profiles may reflect drying of the soils since Pleistocene time (Walvoord and others, 1999).

Chloride concentrations in the unsaturated zone in interdrainage areas were generally high, indicating low water fluxes (fig. 3-4). Maximum chloride concentrations in the Hueco Bolson profiles ranged from 1,858 to 9,343 mg/L. The chloride profiles are generally bulge shaped, with low concentrations near the surface increasing to a maximum at depth and decreasing below the peak to total depth. The bulge has been attributed to higher water fluxes before the last 10,000 yr (during Pleistocene glaciation) and reduction or change from downward to upward flow during the Holocene (~last 10,000 yr). Water fluxes at depth below the bulge in the Hueco Bolson profiles were as much as 0.04 inches/yr (1 mm/yr). Chloride profiles in the sand-sheet areas of Eagle Flat

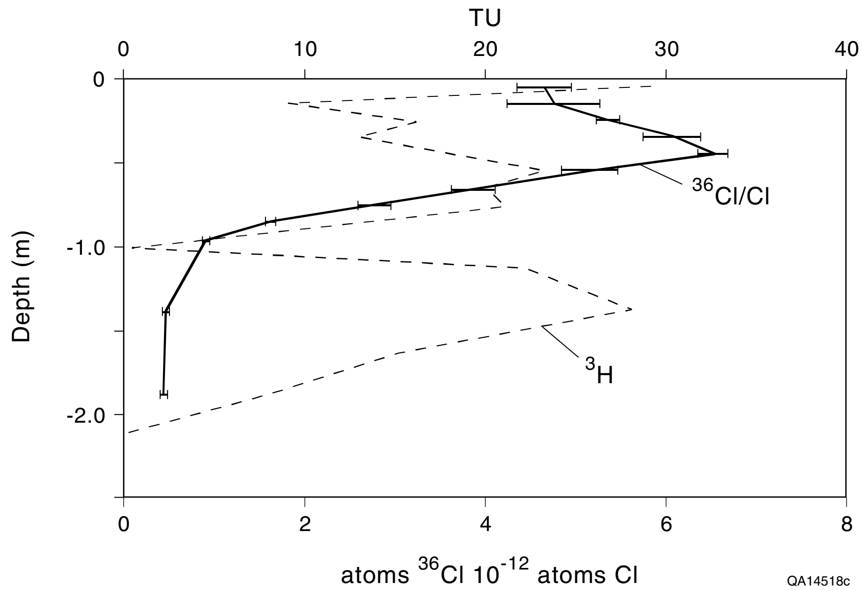

Figure 3-5: Vertical profile of ^{36}Cl:Cl ratios in samples from borehole 51 and ^{3}H concentrations in samples from borehole 52 (Hueco Bolson).

Basin were similar to those in the Hueco Bolson, with maximum chloride concentrations ranging from 1,716 to 7,831 mg/L. Higher chloride concentrations (maximum concentrations in profiles: 5,912 to 17,821 mg/L) were found in the finer grained sediments in interdrainage areas of the Eagle Flat Basin. The age of the water in these profiles was as much as 130,000 yr at a depth of 25 m. Many of these profiles seem to show no response to Pleistocene climate change and remained uniformly high during that time. The calculated age of the water is consistent with dating results from radioactive decay of ^{36}Cl in an interdrainage profile.

Because water ponds in Grayton Lake and was ponded during the study for about 1 yr, chloride concentrations were expected to be negligible, but they were higher. All three chloride profiles in Grayton Lake were bulge shaped, and peak concentrations ranged from 1,084 to 1,315 mg/L. These concentrations indicate low water fluxes (~ 0.01 inches/yr [0.25 mm/yr]), which are attributed to the fine-grained sediments beneath the playa lake. Low chloride concentrations were found beneath the ephemeral stream setting in Eagle Flat Basin (Blanca Draw) (mean chloride, 349 mg/L), suggesting that chloride was flushed out during ponded conditions.

The depth distribution of bomb-pulse ^{36}Cl :Cl was examined in a small ephemeral stream in Hueco Bolson to determine how deep water migrated during the time between bomb fallout (mid-1950's) and the time of sampling (1989). Bomb-pulse ^{36}Cl :Cl was restricted to the upper 4.1 ft (1.25 m) in the Hueco Bolson site; therefore, water must not have moved deeper than 4.1 ft in the past 35 yr (fig. 3-5). The peak depth was located at 1.6 ft (0.5 m). A water velocity of 0.55 inches/yr (14 mm/yr) was calculated on the basis of the depth of the ^{36}Cl :Cl peak (4.1 ft [0.5 m]) and the time between peak fallout and soil-

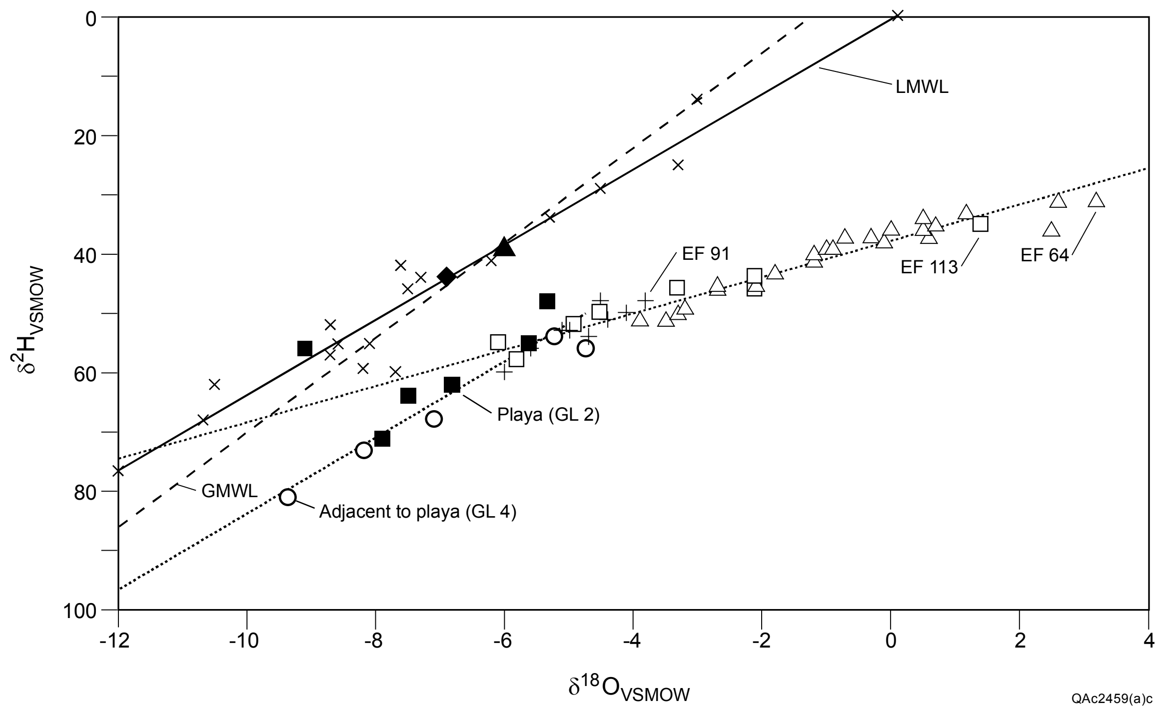

Figure 3-6: Deuterium versus oxygen-18 in soil samples collected beneath Grayton Lake and in interdrainage profiles in Eagle Flat Basin (GMWL, global meteoric water line, LMWL, local meteoric water line).

sample collection (35 yr). The corresponding water flux (0.055 inches/yr [1.4 mm/yr]) was calculated by multiplying water velocity by the average water content in the profile (0.1 ft^3/ft^3). Distribution of bomb-pulse ^3H was also evaluated. The ^3H profile was multipeaked (fig. 3-5), with ^3H concentrations ranging from 23 to 29 TU. The deepest peak (1.4 m) was attributed to the 1963 peak fallout, which resulted in a water velocity of 2.2 inches/yr (56 mm/yr) (assuming a time of 25 yr since peak fallout). The corresponding water flux of 0.28 inches/yr (7 mm/yr) was calculated on the basis of an average volumetric water content of 0.13 ft^3/ft^3. High ^3H concentrations beneath Grayton Lake playa were attributed to preferential flow along desiccation cracks in the floor of the playa.

Stable isotopes of oxygen and hydrogen were used to evaluate subsurface evaporation. A local meteoric water line was estimated from ^{18}O and ^2H data from precipitation that is similar to the global meteoric water line (fig. 3-6). Interdrainage profiles show enrichment of $\delta^{18}O$ relative to δ^2H that is described by $\delta^2H = 3.1\delta^{18}O$. This low slope is consistent with evaporation of pore water in the unsaturated zone. In contrast, stable isotope data from beneath Grayton Lake plot parallel the meteoric water line, indicating negligible evaporation in these sediments.

Recharge on the Diablo Plateau

Results of tritium analysis in groundwater samples in the Diablo Plateau indicate that bomb-pulse tritium was found in most wells in the area (Kreitler and others, 1987). Tritium concentrations ranged from more than 0.8 to 32 TU. Approximately 18 percent of the wells had bomb-pulse tritium (> 0.8 TU). The most likely mechanism for rapid recharge to groundwater is through arroyos and depressions where water ponds at the surface. This hypothesis is supported by the chloride profiles, which were variable in arroyo settings. Low chloride concentrations were measured in one profile (135 mg/L), which corresponds to a water flux of 0.0688 inches/yr (1.75 mm/yr). The other two profiles in arroyo settings had higher chloride concentrations (2,286 to 3,292 mg/L), which resulted in lower water fluxes (0.0041 to 0.0028 inches/yr [0.10 to 0.07 mm/yr]). Low chloride concentrations were also measured in a closed depression (186 mg/L), which corresponds to a water flux of 0.0501 inches/yr (1.27 mm/yr). In contrast, chloride concentrations in interarroyo settings were high in all profiles. Chloride concentrations ranged from 4,211 to 10, 226 mg/L, and calculated water fluxes were low in these settings (0.0022 to 0.0009 inches/yr [0.056 to 0.023 mm/yr]).

Mountain-Front Recharge in Eagle Flat and Red Light Basins

Results of ^{3}H, ^{14}C, and apparent ^{14}C ages of groundwater in Eagle Flat and Red Light Basins are shown in figure 3-7. Average values are shown for wells having multiple samples. The estimated ages are maximum values and are not based on adjustments for the effects of factors that are known to lower the concentrations of ^{14}C in groundwater. In this study, ^{14}C is not regarded as an indicator of absolute age, but of relative age.

The highest ^{3}H and ^{14}C values are found in groundwater along the mountain fronts (adjacent to Eagle Mountain) and where bedrock is exposed or covered by a thin layer of basin-fill sediments. The lowest values of ^{14}C and ^{3}H are found in the deepest groundwater of Eagle Flat and Red Light Basins.

In southeast Eagle Flat Basin, ^{14}C ranges from >107 pmc to 2 pmc, and ^{3}H ranges from 8 to 0 TU. The highest ^{14}C values occur in groundwater of Bean and Millican Hills and the Carrizo and Eagle Mountains. Depth to the potentiometric surface is generally less than 200 ft (<61 m) in these areas, and bedrock is either exposed or covered by a thin layer of basin-fill sediments. The lowest ^{14}C values are consistent with apparent ages that range from 23,000 to 31,000 yr. These age estimates are in line with estimates of recharge ages of groundwater in the Hueco Bolson (Fisher and Mullican, 1990) west of Eagle Flat Basin.

In northwest Eagle Flat, ^{14}C values range from 80.5 to 1.3 pmc, and ^{3}H ranges from 2.0 to 0 TU. The largest concentrations occur in groundwater near the margins of the basin where bedrock of Precambrian or Cretaceous age is exposed. Concentrations of 0 TU are characteristic of deep groundwater near the central area of the flow system.

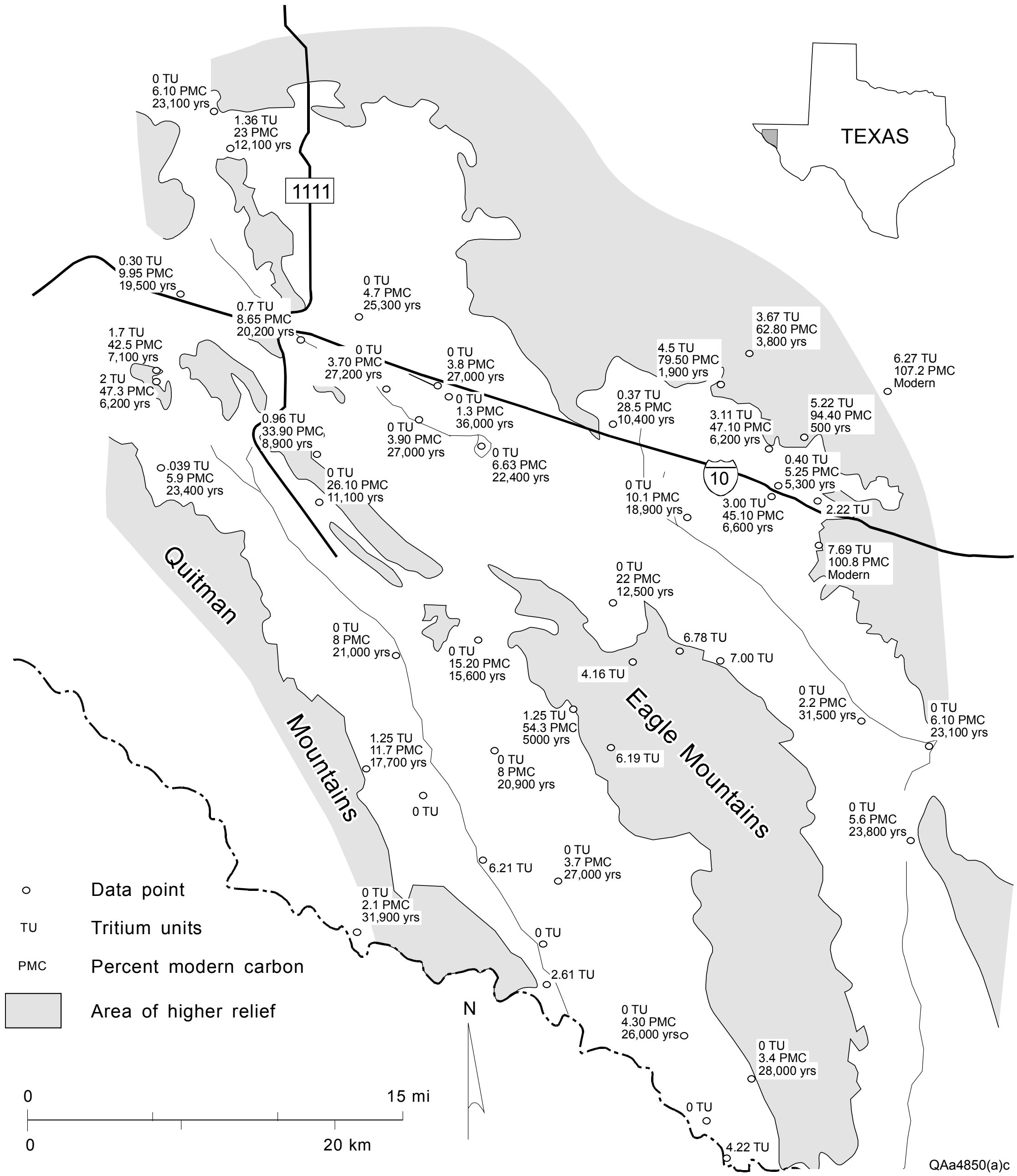

Figure 3-7: Map of groundwater ^{3}H (TU) and ^{14}C (pmc) concentrations and uncorrected ^{14}C ages in Trans-Pecos Texas.

In Red Light Basin, ^{14}C ranges from 54.3 to 2.1 pmc, and ^{3}H ranges from 6.9 to 0 TU. The highest ^{14}C values are associated with wells in the Eagle Mountains and along the northwest part of Devil Ridge. Spatial distribution is one of sharply decreasing ^{14}C with increasing distance from the Eagle Mountains toward the central area of the northwest-oriented basin. For example, ^{14}C decreases from 54.3 to 15.2 pmc or less in wells between the upper and middle alluvial fans of the Eagle Mountains (fig. 3-7). Most ^{14}C concentrations in this area of the basin are less than 8 pmc.

Six wells within Red Light Basin produce groundwater having measurable ^{3}H. The largest values occur in groundwater within the upper elevations of the Eagle Mountains and the upper to middle alluvial fans of the southern Quitman Mountains. Two other wells less than 1 mi north of the Rio Grande produce tritiated groundwater (2.61 and 4.22 TU).

Discussion

Unsaturated-zone studies conducted on the valley floors of the Hueco Bolson and Eagle Flat Basin clearly demonstrate that there is no groundwater recharge in interarroyo settings. Lack of recharge is evidenced by upward water-potential gradients; high chloride concentrations, which result from evapotranspiration, prebomb $^{36}Cl:Cl$ ratios and ^{3}H concentrations below the shallow subsurface; and enrichment in stable isotopes of oxygen and hydrogen relative to the local meteoric water line. Similar results were found in alluvial-fan settings in Ward Valley (California), Amargosa Valley (Beatty, Nevada) (Prudic, 1994) and the Nevada Test Site (Tyler and others, 1996). Chloride concentrations at the Beatty site in Nevada decreased to 50 mg/L at depths more than33 ft (≥10 m), indicating an increase in water flux from 0.25 inches/yr (0.01 mm/yr) (3- to 33-ft zone) to 0.08 inches/yr (2 mm/yr) (>33 ft [10 m] depth). The higher water fluxes at depth were attributed to the Amargosa River being more active during the Pleistocene (Prudic, 1994). Low chloride concentrations at depths of 100 to 197 ft (~30 to 60 m [mean 18 mg/L]) at one of the Nevada Test Site profiles were attributed to the site's location at the confluence of alluvial fans, which affected the system's response to higher precipitation during the Pleistocene.

Recharge occurs primarily on the Diablo Plateau and on the mountain fronts of Eagle Flat and Red Light Basins, judging from the ^{3}H concentrations in groundwater beneath the Diablo Plateau. These are attributed to recharge along arroyos and depressions where water ponds, as shown by chloride profiles. High recharge rates in the mountains and upland areas of Eagle Flat and Red Light Basins are indicated by high ^{3}H concentrations (post-1953 recharge) and high ^{14}C concentrations. Tritium concentrations in deep groundwater in these basins are typically 0 TU, whereas ^{14}C concentrations are low and indicate ages of 20,000 to 30,000 yr. The low ^{14}C values of the deeper groundwater indicate that flow rates within these basins are less than a few feet per year.

Similar results have been found at Yucca Mountain, Nevada: high recharge on the ridge tops and slopes and much lower or no recharge on the valley floors (Flint and others, 2000). The high recharge on the ridge tops and side slopes is attributed to the exposure of fractured rocks near the surface that allows water to migrate rapidly with depth and minimizes evapotranspiration.

Conclusions

Regional evaluation of recharge in the Trans Pecos demonstrates that it occurs primarily in the Diablo Plateau and in the mountains and adjacent areas in Eagle Flat and Red Light Basins and that no recharge occurs in interdrainage areas on the valley floors. High recharge on the Diablo Plateau is evidenced by tritium in groundwater. The primary recharge mechanism is flow in depressions, such as arroyos through fractured rocks, where soils are thin or absent. Deep migration of water minimizes the amount of time that the water resides in the zone of evapotranspiration. High recharge rates in the mountains and adjacent regions and near bedrock exposures in Eagle Flat and Red Light Basins are shown by high ^{3}H and ^{14}C concentrations. In contrast, deep groundwater in these basins typically has 0 TU and low concentrations of ^{14}C, indicating old groundwater (20,000 to 30,000 yr).

Absence of recharge in the interdrainage areas on the valley floors is evidenced by upward water-potential gradients, high chloride concentrations, evapotranspirative enrichment of stable isotopes of oxygen and hydrogen, shallow penetration of bomb-pulse tracers during the past 40 to 50 yr, and radioactive decay of ^{14}C. The water-potential profiles may reflect upward water movement for the past several thousand years during the Holocene and suggest long-term drying of the sediments. The bulge-shaped chloride profiles in the Hueco Bolson indicate higher water fluxes during Pleistocene times (>10,000 yr), with accumulation of chloride since that time. Some of the chloride profiles in the sand-sheet areas of Eagle Flat Basin also showed higher water fluxes during the Pleistocene; however, most of the chloride profiles in Eagle Flat interdrainage areas did not show any response to Pleistocene climate change, probably because the sediments are too fine grained. The drainage areas of the basin floors did show evidence of higher water fluxes, which is attributed to ponding of water in these systems. The size of the drainage systems is important in affecting water fluxes. Small drainages in the Hueco Bolson with low topographic expressions had much higher chloride concentrations and correspondingly lower water fluxes relative to larger drainages in Eagle Flat Basin (e.g., Blanca Draw). Although water fluxes were expected to be high beneath Grayton Lake playa as a result of ponding, the fine-grained sediments in the playa floor effectively reduce water movement through the floor of the playa.

References

Allison, G. B., 1982, The relationship between ^{18}O and deuterium in water in sand columns undergoing evaporation: Journal of Hydrology, v. 55, p. 163-169.

Allison, G. B., Stone, W. J. and Hughes, M. W., 1985, Recharge in karst and dune elements of a semi-arid landscape as indicated by natural isotopes and chloride: Journal of Hydrology, v. 76, p. 1-26.

Bentley, H. W., Phillips, F. M., and Davis, S. N., 1986, ^{36}Cl in the terrestrial environment: *in* Fritz, P., and Fontes, J.-C., eds., Handbook of environmental isotope geochemistry, Elsevier Science, New York, p. 422-475.

Craig, H., 1961, Isotopic variations in meteoric waters: Science, v. 133, p. 1702-1703.

Darling, B. K., 1997, Delineation of the ground-water flow systems of the Eagle Flat and Red Light Basins of Trans-Pecos, Texas: The University of Texas at Austin, Ph.D. dissertation, 179 p.

Fabryka-Martin, J. T., Wightman, S. J., Murphy, W. J., Wickham, M. P., Caffee, M. W., Nimz, G. J., Southon, J. R., and Sharma, P., 1993, Distribution of chlorine-36 in the unsaturated zone at Yucca Mountain−An indicator of fast transport paths: *in* Focus '93: Site characterization and model validation: American Nuclear Society, Las Vegas, Nevada, p. 58-68.

Fisher, R. S., and Mullican, W. F., III, 1990, Integration of ground-water and vadose-zone geochemistry to investigate hydrochemical evolution–a case study in arid lands of the northern Chihuahuan Desert, Trans-Pecos, Texas: The University of Texas at Austin, Bureau of Economic Geology, Geological Circular 90-5, 36 p.

Flint, A. E., Flint, L. E., Hevesi, J. A., D'Agnese, F., and Faunt, C., 2000, Estimation of regional recharge and travel time through the unsaturated zone in arid climates: *in* Faybishenko, B., Witherspoon, P. A., and Benson, S. M., (eds., Dynamics of fluids in fractured rock: American Geophysical Union, Washington, D.C., p. 115-128.

Gat, J. R., 1981, Groundwater: *in* Gat, J. R., and Gonfiantini, R., eds., Stable isotope hydrology, deuterium and oxygen-18 in the water cycle: IAEA, Vienna, Austria, p. 223-240.

Gustavson, T. C., 1990, Regional stratigraphy and geomorphic evolution of the Southern Hueco Bolson, West Texas and Chihuahua, Mexico: *in* Kreitler, C. W., and Sharp, J. M., Jr., eds., Hydrology of Trans-Pecos Texas The University of Texas at Austin, Bureau of Economic Geology, Guidebook 25, p. 27-36.

I.A.E.A., 1983, Isotope techniques in the hydrogeological assessment of potential sites for the disposal of high-level radioactive wastes: *in* IAEA Technical Report Ser. 228, chapter 7, p. 57-61.

King, P. B., 1948, Geology of the southern Guadalupe Mountains, Texas: U.S. Geological Survey Professional Paper 215, 183 p.

Kreitler, C. W., Raney, J. A., Mullican, W. F., III, Collins, E. W., and Nativ, R., 1987, Geologic and hydrologic studies of sites HU1A and HU1B in Hudspeth County, Texas: final report prepared for the Low-Level Radioactive Waste Disposal Authority under contract no. IAC(86-97)-1061, The University of Texas at Austin, Bureau of Economic Geology, 172 p.

Larkin, T. J., and Bomar, G. W., 1983, Climatic atlas of Texas: Texas Department of Water Resources, 151 p.

Mazor, E., 1991, Applied chemical and isotopic groundwater hydrology: Halsted Press, New York, 274 p.

Michel, R. L., 1989, Tritium deposition in the continental United States, 1953-1983: U.S. Geological Survey Water-Resources Investigations Report 89-4072, 46 p.

Phillips, F. M., Mattick, J. L., and Duval, T. A., 1988, Chlorine 36 and tritium from nuclear weapons fallout as tracers for long-term liquid movement in desert soils: Water Resources Research, v. 24, no. 11, p. 1877-1891.

Prudic, D. E., 1994, Estimates of percolation rates and ages of water in unsaturated sediments at two Mojave Desert sites, California-Nevada: U.S. Geological Survey Water Resources Investigation Report 94-4160, 19 p.

Scanlon, B. R., 1992, Environmental and applied tracers as indicators of liquid and vapor transport in the Chihuahuan Desert, Texas: The University of Texas at Austin, Bureau of Economic Geology, Report of Investigations No. 207, 51 p.

Scanlon, B. R., Goldsmith, R. S., and Langford, R. P., 2000, Relationship between arid geomorphic settings and unsaturated zone flow: case study, Chihuahuan Desert, Texas: The University of Texas at Austin, Bureau of Economic Geology, Report of Investigations No. 261, 133 p.

Scanlon, B. R., Wang, F. P., and Richter, B. C., 1991, Field studies and numerical modeling of unsaturated flow in the Chihuahuan Desert, Texas: The University of Texas at Austin, Bureau of Economic Geology, Report of Investigations No. 199, 56 p.

Solomon, D. K., and Sudicky, E. A., 1991, Tritium and helium-3 isotopic ratios for direct estimation of spatial variations in groundwater recharge: Water Resources Research, v. 27, p. 2309-2319.

Tyler, S. W., Chapman, J. B., Conrad, S. H., Hammermeister, D. P., Blout, D. O., Miller, J. J., Sully, M. J., and Ginanni, J. M., 1996, Soil-water flux in the southern Great Basin, United States—Temporal and spatial variations over the last 120,000 years: Water Resources Research, v. 32, p. 1481-1499.

Walvoord, M. A., Phillips, F. M., Plummer, M. A., and Wolfsberg, A., 1999, Thick desert vadose zones—What is the equilibrium state? Geological Society of America, Abstracts with Programs, v. 31, no. 7.